Flora 230 (2017) 66–74

Contents lists available at ScienceDirect

Flora

journal homepage: www.elsevier.com/locate/flora

The velamen of epiphytic orchids: Variation in structure and correlations with nutrient absorption

Thais Arruda Costa Joca [a], Denis Coelho de Oliveira [a], Gerhard Zotz [b,c], Uwe Winkler [b,†], Ana Silvia Franco Pinheiro Moreira [a,*]

[a] Universidade Federal de Uberlândia, Instituto de Biologia, Rua Ceará s/n, Bloco 2D, Campus Umuarama, CEP 38400-902, Uberlândia, MG, Brazil
[b] Universität Oldenburg, Institute for Biology and Environmental Sciences, Oldenburg, Germany
[c] Smithsonian Tropical Research Institute, Balboa, Panama

ARTICLE INFO

Article history:
Received 6 October 2016
Received in revised form 7 March 2017
Accepted 13 March 2017
Edited by Hermann Heilmeier
Available online 16 March 2017

Keywords:
Nutrient uptake
Orchidaceae
Passage cells
Pectins
Root anatomy
Velamen structure

ABSTRACT

Roots of epiphytic orchids typically possess a velamen radicum, a multiple epidermis composed of dead cells. It is largely unexplored how the structure of the velamen, the cortex and vascular cylinder facilitate the flow of water and nutrients towards the plant. Up to now, structural root features were rarely correlated with functional attributes. In this study, we compare anatomical features with nutrient uptake rates (specifically of phosphorus and rubidium) of roots of 18 taxa of epiphytic orchids. The relative proportion of the velamen of the cross-sectional area varied from 11 to 97%. Species with the largest relative velamen area facilitate the flow of water and nutrients, and species with larger relative proportion of vascular cylinder and cortex have a greater number of protoxylem strands and passage cells of the endodermis. The number of passage cells in the endodermis and of differential wall thickenings in cortical cells may play an important role in apoplastic and symplastic flow. The velamen pectic matrix, with negative charge, can retain cations (like Rb^+), while a higher number of strands in the xylem, aligned with passage cells of the endodermis, could facilitate the entry of these ions into the vascular cylinder.

1. Introduction

The epiphytic environment imposes a number of restrictions to plants. Many of the anatomical features commonly found among epiphytes are related to the uptake of water and nutrients, such as absorbing scales in the Bromeliaceae or the velamen radicum in Orchidaceae (Withner, 1959; Benzing, 1990; Zotz and Hietz, 2001; Laube and Zotz, 2003). Although the availability of water and nutrients is sporadic and depends on atmospheric sources (Benzing, 1990), growth in tree crowns ensures an environment with an improved supply of light (Tsavkelova et al., 2001). It is known that approximately 10% of all vascular plants are epiphytes, the Orchidaceae being particularly noteworthy because around 70% of all species are epiphytic (Zotz, 2013). This success in tree crowns is arguably due to anatomical and physiological strategies that compensate for the scarcity of water and nutrients, promoting in the effective absorption and use of these resources when intermittently available (Scatena and Nunes, 1996).

Among the adaptive features of orchid roots, the presence of velamen stands out (Zotz and Hietz, 2001). The velamen is located externally to the exodermis, the outer layer of the cortex, and constitutes a multiple epidermis composed of dead cells (Pridgeon, 1987). Initially, Went (1940) proposed an important role of the velamen in capturing and immobilizing solutions that arrive at the root via stem flow, and recent experimental evidence provides support for this notion (Zotz and Winkler, 2013). In addition to the function of water absorption, the velamen also reduces the loss of water at times of low availability of water and confers mechanical protection for the root (Pridgeon, 1987; Benzing, 1996).

Internally to the velamen, the cortex consists of parenchymatic cells. In Orchidaceae there are different types of parietal thickenings, i.e. reticulated, uniform or phi forms (Stern, 1999; Stern and Judd, 2001; Moreira et al., 2013). The exodermis and endodermis (outermost and innermost layers of the cortex, respectively) delineate the cortical parenchyma in these roots, and the presence of an endodermis acts as boundary between the cortex and the vascular cylinder. Exodermis and endodermis are formed by cells that can have Casparian strips, be highly lignified and sometimes dead at maturity, alternating with passage cells which remain alive

* Corresponding author.
E-mail addresses: thais_arrudacj@hotmail.com (T.A.C. Joca), denisoliveira@inbio.ufu.br (D.C. de Oliveira), gerhard.zotz@uni-oldenburg.de (G. Zotz), anasilviamoreira@gmail.com (A.S.F.P. Moreira).
[1] In memorian

http://dx.doi.org/10.1016/j.flora.2017.03.009
0367-2530/

(Pridgeon, 1987; Trépanier et al., 2008). The lignified cells (or with Casparian strips) in these layers act as a barrier for the movement of ions and other substances through the apoplast (Esnault et al., 1994; Ma and Peterson, 2003), while the passage cells are the main cells capable of symplastic movement (Peterson and Enstone, 1996). These cells allow water and nutrient absorption (Peterson and Enstone, 1996), and are responsible for the selectivity of solutes to be transported to the vascular cylinder (Peterson, 1988; Trépanier et al., 2008).

This study wants to relate the investment of Orchidaceae roots in velamen and/or in other internal structures to the functions assigned to the passage cells and velamen found in the cited literature, specifically the absorption of nutrients. We focus on the relationship of the thickness of the velamen and the number of passage cells (of both the endodermis and exodermis) as structural characteristics on the one hand and the rate of absorption of phosphorus and rubidium on the other hand for a set of 18 taxa of epiphytic orchids.

2. Material and methods

Individuals of *Bifrenaria harrisoniae* (Hook.) Rchb.f., *Catasetum planiceps* Lindl., *Cattleya skinneri* Bateman *alba*, *Caularthron bilamellatum* (Rchb.f.) R.E. Schult, *Dendrobium fimbriatum* Hooker, *Dendrobium nobile* Lindl., *Dendrobium nobile* hybrid, *Dimerandra emarginata* (G. Mey.) Hoehne, *Doritis pulcherrima* Lindl., *Encyclia ghillanyi* Pabst, *Epidendrum ciliare* L., *Epidendrum nocturnum* Jacq., *Gongora unicolor* Schltr., *Miltonia bluntii* Rchb.f., *Phalaenopsis cornu-cervie* Blume & Rchb.f., *Phalaenopsis* hybrid, *Oncidium* sp. and *Trichoglottis bipunctata* (C.S.PP. Parish & Rchb.f.) Tang & F.T. Wang were obtained from the Botanical Garden of the University of Marburg (Germany) or from collections in Panama, and acclimated in a greenhouse of the University of Oldenburg (Germany), at a temperature of 26/20 °C (day/night) and a relative humidity of ca. 65%. Fragments of aerial roots were submitted to tests of nutrients absorption (phosphorus and rubidium) in the Radionuclide Laboratory of the University of Oldenburg and parallel samples were fixed in 4% paraformaldehyde (Roland and Vian, 1991). The anatomical analyses were performed in the Laboratory of Plant Anatomy and Development of the Universidade Federal de Uberlândia, Brazil.

2.1. Experiments of nutrient absorption

Nutrient absorption was assayed similar to the procedure described in Zotz and Winkler (2013) using the following radioisotopes: carrier free ^{32}P phosphoric acid (Hartmann Analytic, Germany), containing 37 MBq in 100 μl water (initial specific activity: 5.5 MBq nmol^{-1} ^{32}P); aquatic solutions of $^{86}RbCl$ (Hartmann Analytic, Germany) with a specific activity of 720 MBq mg^{-1} Rb^+ and aquatic solutions of [^{14}C(U)-D-glucose] with a specific activity of 13.3 GBq mmol^{-1}. The radioisotope of rubidium is a well-established analytical analogue for potassium, because the uptake kinetics of K^+ and Rb^+ are generally comparable (Läuchli and Epstein, 1970). Aliquots of labelled substances with an initial activity of 0.15 mBq in 5 ml incubation solution were used in uptake experiments with the 18 different taxa. The uptake of phosphate was measured in solutions containing radioactive labelled ^{32}P phosphate and unlabelled phosphate to give a final substrate concentration of 15 μM. Radioactive, labelled ^{86}Rb and unlabelled RbCl were mixed to obtain a similar final concentration of 15 μM. Such concentrations are within the range of concentrations naturally occurring in rainwater (e.g. Benzing, 2000).

Four root segments of each taxon, excised at 4 cm from the root tip, were submerged in solutions of incubation in test tubes, and absorption rates were determined by the decrease of the radioactivity in aliquots of 10 μl of the solutions of incubation (with pH 6.1) after standardizing the volume of liquid, adding the solution not labelled to the initial volume of incubation, mixing with Pasteur pipettes. The velamen was removed just above the submerged portion to prevent the passive diffusion in this tissue.

The cumulative absorption of phosphate and rubidium was calculated from the decrease of the radioactivity in the solution of incubation with a constant volume, according to the following equation:

$$Absorption(\text{nmol}) = P_\Sigma - (dpm_{t0}/dpm_{t1} \times P_\Sigma),$$

where P_Σ is the initial quantity of substrate in the solution (nmol); dpm_{t0} is the counting rate in 10 μl at beginning of absorption and DPM_{t1} the counting rate in 10 μl at the end of the period of absorption. The rates were expressed against root length (cm).

2.2. Structural analysis

For anatomical comparisons of the roots, histological slides of transverse hand cuts were prepared 3 cm from the apex. The material was clarified in 50% sodium hypochlorite (Kraus and Arduin, 1997) and stained with 1% alcoholic solution of safranin and 0.5% Astra blue (1:9 v/v) (Bukatsch, 1972). The slides were assembled with gelatin glycerinated of Kaiser (Johansen, 1940) and the material photographed under light microscope Leica® DM500 equipped with digital camera Leica® ICC50 HD.

For each species, four individuals were analyzed when available (see analysis of results). For each individual, 15 transverse cuts were performed. The diameter, the number of layers, the thickness and the cross-sectional area occupied by the velamen, and the cross-sectional areas of vascular cylinder and the cortex were determined at three different points of a given cut. The cross-sectional areas of different tissue types were expressed relative to the total area. The total number of cells of the exodermis and endodermis, the thickness of the cell walls of the exodermic cells and the number of passage cells were quantified as were the ratios of passage cells to the other cell components of the endodermis and exodermis. In addition, we counted the number of strands of xylem and phloem. For all counts and measurements, IMAGE J 1.x software (National Institute of Health, USA) was used.

2.3. Histochemical analysis

The presence of proteins was used to identify living cells and tissues. Transverse sections were incubated in 1% bromophenol blue solution (w/v) for 10–15 min (Durrum, 1950), washed in 50% ethanol (v/v) and assembled in distilled and deionized water. Pectins were detected incubating transverse sections in 50% ethanol, and staining with 0.2% ruthenium red (w/v) for 10 min (Chamberlain, 1932; modified).

2.4. Data analysis

Structural data were analyzed with the averages of the individuals in each species. For *Caularthron bilamellatum, Cattleya skinneri alba, Dendrobium fimbriatum, Epidendrum ciliare* and *Miltonia bluntii*, there was only material available from a single individual. For *Phalaenopsis* hybrid, *Gongora unicolor* and *Trichoglottis bipunctata* there were only two available individuals of each taxon. In all other cases, four individuals were used.

We evaluated the correlation between variables using Pearson test for parametric data. The same test was used to compare the structural characteristics with the rates of absorption of rubidium and phosphorus. All tests were performed using SYSTAT 10.2 soft-

ware (SPSS, 2000, San Francisco). A level of $P < 0.05$ was interpreted as significant.

3. Results

3.1. Root morphology and anatomy

The structure of the roots of the 18 analyzed taxa was qualitatively similar (for a typical example see Fig. 1A) although the velamen differed fourfold in the number of cell layers (3–11 layers of dead cells, Table 1) and the patterns of parietal thickenings varied as well. Parietal thickenings in the cortical parenchyma were lacking in most species (Table 2), while eight species had some parenchymatic cells with conspicuously cell wall-thickenings of three different types; either reticulated (Fig. 1B), uniform (Fig. 1C) or phi (Fig. 1D and E). Noteworthy, in a few cases we found variation even within a species. Cells with reticulated thickenings were found in *Bifrenaria harrisoniae* in one of the roots of a single individual, while cells with uniform thickenings were found in all the other roots of this species. *Cattleya skinneri alba* showed cells with prominent phi-thickening throughout the cortex in all the roots, while in *Catasetum planiceps*, this type of thickening was only found in three roots out of seven analyzed. In this species, some roots showed phi-thickening encircling the entire cortex, while in other roots, the phi-thickening was interrupted. In *Encyclia ghillanyi*, phi-thickening was slightly prominent in only one of the roots. In *Trichoglottis bipunctata*, the reticulated thickening was found in all the roots. Most cells of the exodermis and endodermis, which delimit the cortical parenchyma, are dead, with walls showing different degrees of thickening, interspersed by passage cells. The strands of xylem and phloem are intercalated in the vascular cylinder and immersed in parenchymatic cells that show centripetal sclerification (Fig. 1F and G). Histochemical tests showed that only the passage cells in the exodermis (Fig. 2A) and endodermis are alive, and the velamen maintains the same pectic structure even at maturity (Fig. 2B).

Some species had a very well developed velamen (Fig. 3A), while in others cortex and vascular cylinder dominated the transversal area of the root. There was a continuous variation from species with very large to species with very small proportions of the velamen, the extreme values being 97% (*Catasetum planiceps*, Table 2) and 11% (*Phalaenopsis cornu-cervie*, Table 2, Fig. 3B) of the area of a cross section of the roots occupied by this tissue.

In relation to the ratio of the number of passage cells with the number of the thickened cells of the exodermis (Table 1), interspecific differences were relatively small, with values between 0.1 and 0.3. The same was observed for the endodermis, which presented values between 0.2 and 0.6. The smallest ratios were found in *Phalaenopsis* hybrid, *Doritis pulcherrima* and *Phalaenopsis cornu-cervie*.

Endodermis and exodermis had the same type of "O" or "U"-thickenings for all the analyzed sections of a given taxon. The endodermis had "O" thickening for all the taxa evaluated (Fig. 3C), and this was also true for the exodermis of most species (Fig. 3D). "U"-thickening of the cell walls in the exodermis were observed only for *Phalaenopsis* hybrid, *Epidendrum ciliare* (Fig. 3E), *E. nocturnum* and *Doritis pulcherrima*. Regarding the cell wall thickness types of the exodermis, it was possible to observe species with less prominent thickenings – as in *Bifrenaria harrisoniae*, *Catasetum planiceps*, *Dendrobium nobile*, *Dendrobium nobile* hybrid, *Dimerandra emarginata*, *Doritis pulcherrima*, *Encyclia ghillanyi* (Fig. 3F), *Epidendrum nocturnum*, *Gongora unicolor*, *Miltonia bluntii*, *Oncidium* sp. and *Phalaenopsis cornu-cervie*; and species with more pronounced thickenings – i.e. in *Caularthron bilamellatum*, *Cattleya skinneri alba*, *Dendrobium fimbriatum* (Fig. 3D), *Epidendrum ciliare* (Fig. 3E), *Phalaenopsis* hybrid and *Trichoglottis bipunctata*.

Table 1
Structural characteristics of roots from 18 taxa of epiphytic orchids. Data are means ± SD of 15 cuts in each replicate available for each species.

	Root diameter (mm)	Root area in cross section (mm^2)	Number of layers of the velamen	Thickness of velamen (µm)	Velamen area in cross section (mm^2)	Number of lignified cells of the exodermis	Number of passage cells of the exodermis	Ratio of passage cells to total cells of the exodermis	Cortex thickness (µm)	Number of lignified cells of the endodermis	Number of passage cells of the endodermis	Ratio of passage cells to total cells of the endodermis	Number of protoxylem strands	Vascular cylinder+cortex area (mm^2)
Bifrenaria harrisoniae	4.3 ± 0.5	14.6 ± 3.0	8.0 ± 0.5	853.0 ± 147	9.2 ± 2.4	200.2 ± 4.0	51.1 ± 4.0	0.26	1018.2 ± 95.3	126.6 ± 15.6	50.6 ± 7.5	0.40	18.9 ± 0.8	5.4 ± 1.0
Catasetum planiceps	2.8 ± 0.4	6.9 ± 1.5	11.1 ± 0.6	921.8 ± 61	6.7 ± 2.0	134.5 ± 6.5	25.0 ± 0.7	0.19	712.8 ± 42.2	78.4 ± 5.6	48.6 ± 0.3	0.62	11.4 ± 0.5	0.2 ± 0.5
Cattleya skinneri alba	2.1 ± 0.1	3.5 ± 0.3	5.5 ± 0.3	503.6 ± 94	2.5 ± 0.4	182.2 ± 18.3	38.0 ± 3.8	0.21	567.8 ± 58.3	88.8 ± 4.3	35.6 ± 4.4	0.40	13.5 ± 0.6	1.0 ± 0.4
Caularthron bilamellatum	1.4 ± 0.2	1.7 ± 0.6	5.2 ± 0.8	248.8 ± 79	0.9 ± 0.2	121.2 ± 13.9	29.3 ± 6.4	0.24	297.4 ± 65.6	82.2 ± 21.1	38.3 ± 9.4	0.47	14.4 ± 5.0	0.80 ± 0.6
Dendrobium fimbriatum	2.2 ± 0.1	3.7 ± 0.5	10.1 ± 0.6	525.8 ± 47	2.7 ± 0.3	165.5 ± 8.4	19.0 ± 5.3	0.11	305.1 ± 16.0	108.9 ± 6.3	48.2 ± 3.3	0.44	15.2 ± 0.8	1.0 ± 0.2
Dendrobium nobile	1.8 ± 0.9	2.5 ± 0.2	6.9 ± 0.6	463.4 ± 28	1.9 ± 0.2	153.1 ± 12.3	31.5 ± 6.1	0.21	324.7 ± 6.6	81.0 ± 7.6	32.8 ± 2.8	0.41	9.5 ± 0.9	0.6 ± 0.1
Dendrobium nobile hybrid	1.6 ± 0.3	2.1 ± 0.6	7.4 ± 0.2	409.9 ± 89	1.6 ± 0.5	150.4 ± 19.8	36.8 ± 2.4	0.25	301.6 ± 20.7	78.9 ± 7.4	31.2 ± 3.11	0.40	9.2 ± 0.9	0.5 ± 0.1
Dimerandra emarginata	2.7 ± 0.2	6.0 ± 1.1	3.9 ± 0.4	198.8 ± 33	1.6 ± 0.4	196.6 ± 16.3	45.5 ± 5.4	0.23	1123.8 ± 92.8	73.9 ± 11.7	20.8 ± 6.4	0.28	11.3 ± 3.0	4.4 ± 0.7
Doritis pulcherrima	2.4 ± 0.1	4.5 ± 0.5	3.1 ± 0.1	123.4 ± 6	0.9 ± 0.04	194.0 ± 14.6	46.9 ± 3.4	0.24	1309.0 ± 127.2	55.1 ± 2.6	11.6 ± 0.3	0.21	7.6 ± 0.1	3.6 ± 0.5
Encyclia ghillanyi	1.3 ± 0.1	1.5 ± 0.2	6.5 ± 0.3	282.6 ± 43	0.9 ± 0.9	90.4 ± 2.9	24.1 ± 1.2	0.27	282.8 ± 48.1	73.5 ± 1.7	30.3 ± 1.5	0.41	10.8 ± 0.5	0.6 ± 0.1
Epidendrum ciliare	2.4 ± 0.5	4.7 ± 1.9	5.4 ± 0.7	410.5 ± 80	2.6 ± 0.9	225.2 ± 50.2	47.6 ± 14.9	0.21	730.6 ± 135.2	105.2 ± 17.2	40.4 ± 11.2	0.38	18.0 ± 1.0	2.1 ± 1.2
Epidendrum nocturnum	3.1 ± 0.2	7.5 ± 0.8	4.0 ± 0.2	212.0 ± 24	1.9 ± 0.2	219.4 ± 26.0	54.5 ± 3.6	0.25	1174.3 ± 84.7	94.5 ± 12.5	27.3 ± 1.9	0.29	12.0 ± 0.7	5.6 ± 0.6
Gongora unicolor	1.2 ± 0.1	1.1 ± 0.2	6.2 ± 0.5	303.7 ± 18	0.8 ± 0.04	60.8 ± 0.5	19.3 ± 0.6	0.32	239.7 ± 14.1	47.5 ± 0.2	19.1 ± 0.9	0.40	7.2 ± 0.2	0.3 ± 0.1
Miltonia bluntii	2.4 ± 0.2	1.1 ± 0.3	7.3 ± 1.6	321.1 ± 78	0.8 ± 0.2	66.1 ± 10.9	18.8 ± 3.1	0.29	183.5 ± 25.4	60.5 ± 9.4	19.3 ± 4.2	0.32	7.4 ± 1.6	0.3 ± 0.2
Phalaenopsis cornu-cervie	4.5 ± 0.7	20.0 ± 4.8	3.1 ± 0.1	134.4 ± 13	2.1 ± 0.4	294.7 ± 62.5	69.4 ± 5.0	0.24	1961.3 ± 238.0	92.6 ± 23.1	20.0 ± 3.3	0.22	13.2 ± 1.8	17.9 ± 4.4
Phalaenopsis hybrid	5.8 ± 0.3	26.3 ± 3.0	3.1 ± 0.01	169.1 ± 2	3.0 ± 0.2	404.3 ± 24.1	112.1 ± 2.6	0.28	2282.1 ± 242.6	142.7 ± 6.5	27.4 ± 1.7	0.19	22.2 ± 1.2	23.3 ± 2.8
Oncidium sp.	1.5 ± 0.3	1.2 ± 0.2	7.0 ± 0.3	403.9 ± 51	1.0 ± 0.09	76.3 ± 23.3	22.2 ± 5.0	0.30	198.5 ± 7.1	59.5 ± 9.7	19.6 ± 5.7	0.33	8.0 ± 1.8	0.2 ± 0.2
Trichoglottis bipunctata	1.4 ± 0.2	1.5 ± 0.4	6.8 ± 0.3	297.5 ± 42	1.0 ± 0.3	132.8 ± 13.3	31.0 ± 1.5	0.23	325.5 ± 46.2	70.5 ± 8.1	25.3 ± 3.0	0.36	10.2 ± 0.9	0.5 ± 0.1

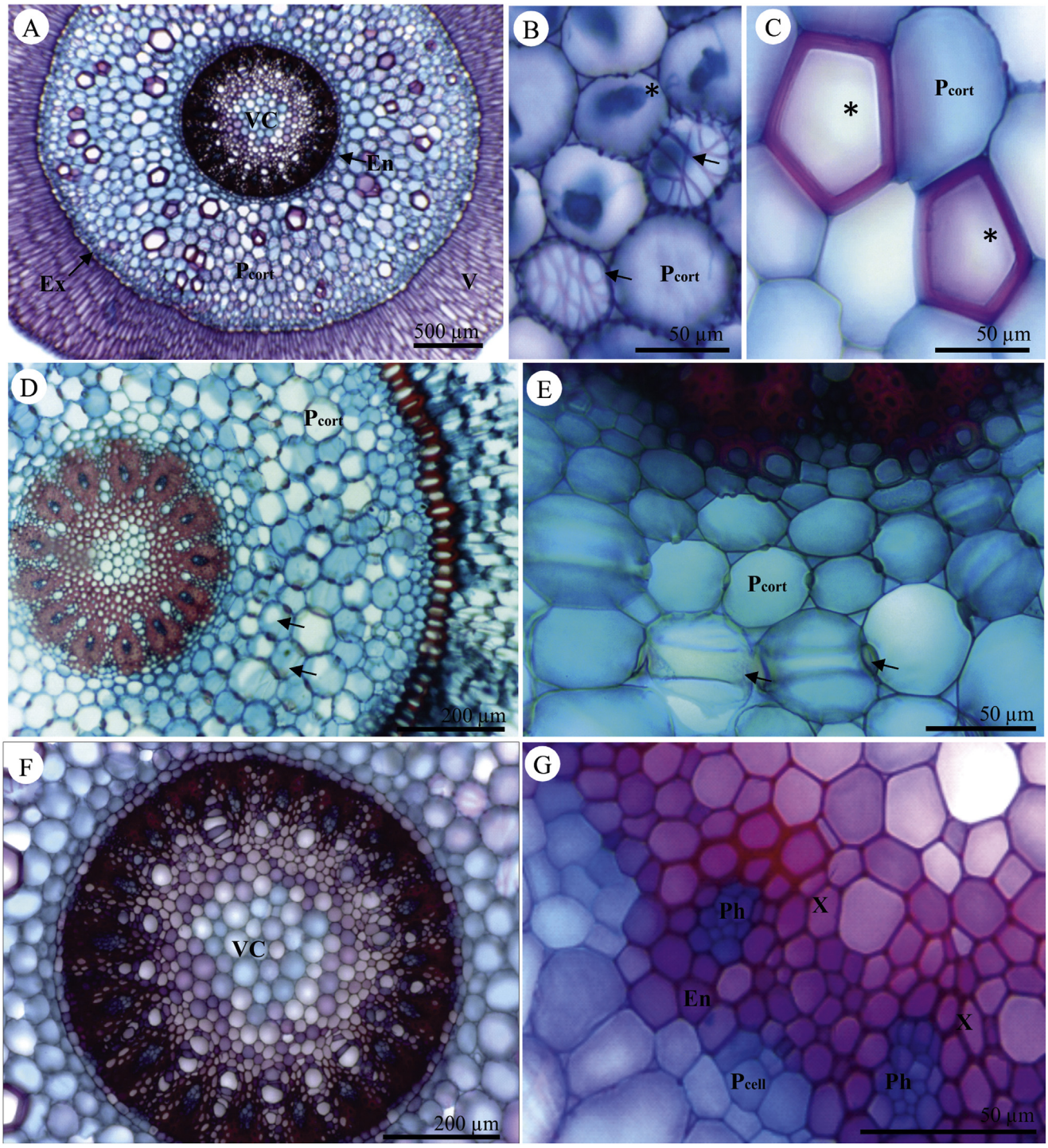

Fig. 1. Transverse sections of orchid roots. (A) *Bifrenaria harrisoniae*, overview showing velamen, exodermis and endodermis delimiting the cortical parenchyma and the vascular cylinder. (B) *Catasetum planiceps*, detail of cortical cells with reticulated thickening (arrows) and mycorrhizal peletons (*). (C) *Bifrenaria harrisoniae*, detail of cortical cells with uniform thickening (*). (D and E) *Cattleya skinneri alba*, (D) distribution and (E) detail of phi-thickening (arrows) in cortical parenchyma. (F) *Bifrenaria harrisoniae*, vascular cylinder with strands of xylem and intercalated phloem, and centripetal sclerification of medullary parenchyma. (G) *Catasetum planiceps*, detail of the vascular cylinder. En = endodermis; Ex = exodermis; Ph = phloem; Pcell = passage cell; Pcort = cortical parenchyma; V = velamen; VC = vascular cylinder; X = xylem.

The number of protoxylem strands mostly varied from 7.2 (in *Gongora unicolor*) to 14.4 (in *Caularthron bilamellatum*) (Table 1). However, two species (*Bifrenaria harrisoniae* and *Phalaenopsis* hybrid) showed substantially larger numbers with 18.9 and 22.2 protoxylem strands, respectively.

3.2. Correlation between anatomical traits and the rate of Rb and P_i absorption

We found a number of correlations between anatomical characteristics (Table 3). Among these, we highlight the correlation between root cross sectional area (or root diameter, since the area was calculated from the diameter) with the area occupied by the

Table 2
Type of wall thickenings and thickness of exodermis and endodermis cells, and tissue proportions of roots for 18 taxa of epiphytic orchids. Data are means ± SD of 15 cuts in each replicates available of each species.

	Type of wall thickening of the exodermis cells	Type of wall thickening of the endodermis cells	Thickness of cell wall of the cells of the exodermis (mm)	Proportion of the velamen area to the total area of the root	Proportion of the vascular cylinder + cortex area to the total	area of the root
Bifrenaria harrisoniae	O	O	2.84 ± 0.1	ret; unif	63.0%	37.0%
Catasetum planiceps	O	O	2.77 ± 0.4	ret; phi	97.1%	2.9%
Cattleya skinneri alba	O	O	8.29 ± 1.3	Phi	71.4%	28.6%
Caularthron belamellatum	O	O	10.09 ± 1.7	–	52.9%	47.1%
Dendrobium fimbriatum	O	O	6.77 ± 1.7	–	73.0%	27.0%
Dendrobium nobile	O	O	4.77 ± 0.4	Unif	76.0%	24.0%
Dendrobium nobile hybrid	O	O	4.90 ± 0.7	–	76.2%	23.8%
Dimerandra emarginata	O	O	4.58 ± 0.4	–	26.7%	73.3%
Doritis pulcherrima	U	O	4.31 ± 0.5	–	20.0%	80.0%
Encyclia ghillanyi	O	O	2.94 ± 0.1	Phi	60.0%	40.0%
Epidendrum ciliare	U	O	11.18 ± 3.1	–	55.3%	44.7%
Epidendrum nocturnum	U	O	4.79 ± 0.4	–	25.3%	74.7%
Gongora unicolor	O	O	2.91 ± 0.2	–	72.7%	27.3%
Miltonia bluntii	O	O	4.22 ± 1.0	Unif	72.7%	27.3%
Oncidium sp.	O	O	3.40 ± 0.6	Unif	83.3%	16.7%
Phalaenopsis cornu-cervie	O	O	4.38 ± 0.1	–	10.5%	89.5%
Phalaenopsis hybrid	U	O	9.15 ± 0.1	–	11.4%	88.6%
Trichoglottis bipunctata	O	O	6.37 ± 1.4	Ret	66.7%	33.3%

In the type of wall thickening of the cells of the cortical parenchyma, the abbreviation (ret) is reticulated, (unif) is uniform and (phi) is phi-thickening.

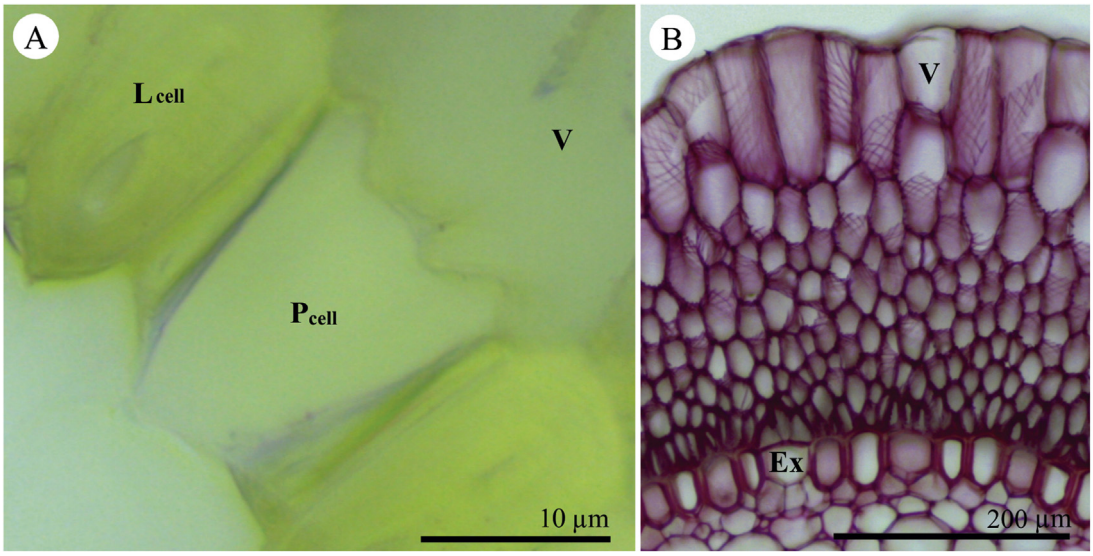

Fig. 2. Histochemical analyses. (A) *Caularthron bilamellatum*, detail of the exodermis with one passage cell stained with bromophenol blue, showing proteins in the protoplast, the other cells being lignified with massive wall thickening and reduced lumen. (B) *Trichoglottis bipunctata*, stained with ruthenium red showing pectic impregnation, including parietal thickenings in velamen cells. Lcell = lignified cells; Ex = exodermis; Pcell = passage cell; V = velamen.

vascular cylinder and cortex ($r = 0.96$, $p < 0.001$), with the number of protoxylem strands ($r = 0.70$, $p < 0.001$) and with the number of passage cells of the exodermis ($r = 0.90$, $p < 0.001$). Characteristics of velamen such as the area occupied in cross-section, the number of cell layers and total thickness, in turn, showed significant positive correlations with characters related to the water transport inside the root (such as the number of passage cells of the endodermis and the number of protoxylem strands). On the other hand, the number of passage cells of the exodermis was negatively correlated with the number of cell layers of the velamen ($r = -0.64$, $p < 0.001$). The number of layers of velamen cells was negatively correlated with the area occupied by the vascular cylinder and cortex ($r = -0.56$, $p < 0.005$), the thickness of the cortex ($r = -0.63$, $p < 0.001$) and the thickness of the cell wall of the exodermis ($r = -0.29$, $p < 0.001$).

Cortex thickness was positively correlated with the number of protoxylem strands ($r = 0.54$, $p < 0.005$) and with the number of passage cells of the exodermis ($r = 0.93$, $p < 0.001$). When analyzing the number of strands of protoxylem, three positive correlations were relevant: the greater the number of vascular strands, the greater the number of passage cells of the exodermis ($r = 0.67$, $p < 0.001$), the number of passage cells of the endodermis ($r = 0.57$, $p < 0.001$) and the thickness of cell walls from exodermis ($r = 0.59$, $p < 0.001$).

Correlations were found, although rather weak, between the rates of absorption of rubidium and the cross-sectional area of the velamen ($r^2 = 0.33$, $p < 0.01$), with the number of protoxylem strands ($r^2 = 0.28$, $p < 0.02$), with the number of passage cells of the endodermis ($r^2 = 0.21$, $p < 0.05$), and are represented in Fig. 4. No correlation was observed between any anatomic variable and the rates of phosphorus absorption.

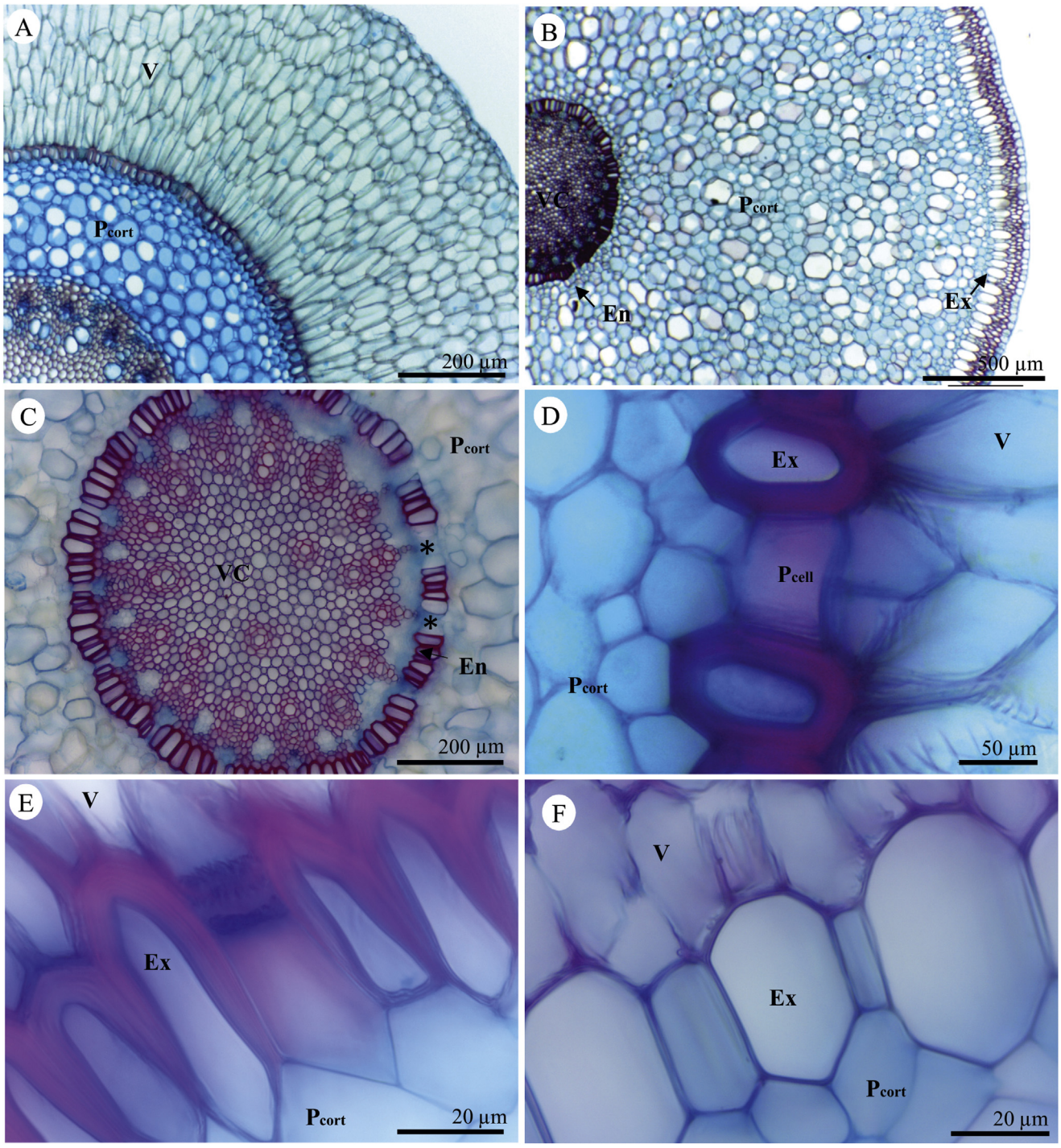

Fig. 3. Transverse sections of Orchidaceae roots. (A) *Dendrobium fimbriatum*, general view showing extensive velamen. (B) *Phalaenopsis cornu-cervie*, general view showing greater area corresponding to the cortex and vascular cylinder. (C) *Phalaenopsis cornu-cervie*, vascular cylinder surrounded by endodermis with O-thickening and passage cells (*). (D) *Dendrobium fimbriatum*, detail of exodermis with O-thickenings and passage cell. (E) *Epidendrum ciliare*, exodermis with U-thickening and passage cell. (F) *Encyclia ghillanyi*, exodermis with thin walled cells. En = endodermis; Ex = exodermis; Pcell = passage cell; Pcort = cortical parenchyma; V = velamen; VC = vascular cylinder.

4. Discussion

4.1. Functional anatomy of epiphytic roots

The studied roots of epiphytic orchids seem to invest in two paths to ensure effectiveness in water and nutrient absorption: greater proportion of velamen, or a greater number of protoxylem strands and passage cells of endodermis in species with larger areas of the vascular cylinder and cortex. Up to now, structural features of roots are discussed in an independent manner, without any correlation among themselves (Peterson and Enstone, 1996; Moreira and Isaias, 2008). Functionally, the velamen is taken as a facilitator in water and nutrient absorption, barrier to loss of water and capable of conferring mechanical resistance (Pridgeon, 1987; Benzing et al., 1982). However, the analysis of the relation between the velamen and the different layers of the cortex and vascular cylinder helps to identify possible trade-offs and to understand which structural strategies are more effective to maximize the water and

Table 3
Matrix of correlation coefficients between anatomical characteristics of roots of 18 orchid taxa. The measurements were performed in 15 transversal cuts of each individual available for each taxon. The data reflect the correlations between averages.

1	2	3	4	5	6	7	8	9	10	11	12	13	
-	0.97*	0.51*	0.90*	-0.34^{ns}	-0.01^{ns}	0.90*	0.69*	0.86*	0.87*	0.74*	0.09^{ns}	0.10^{ns}	**1**
	-	0.44^{ns}	0.96*	-0.39^{ns}	-0.08^{ns}	0.91*	0.70*	0.88*	0.90*	0.74*	0.06^{ns}	0.12^{ns}	**2**
		-	0.16^{ns}	0.44^{ns}	0.81*	0.24^{ns}	0.53*	0.26^{ns}	0.19^{ns}	0.57*	0.71*	-0.18^{ns}	**3**
			-	-0.56*	-0.35^{ns}	0.93*	0.59*	0.89*	0.93*	0.62*	-0.17^{ns}	0.19^{ns}	**4**
				-	0.83*	-0.63*	-0.12^{ns}	-0.54*	-0.64*	-0.06^{ns}	0.64*	-0.29*	**5**
						-0.31^{ns}	0.18^{ns}	-0.23^{ns}	-0.33^{ns}	0.22^{ns}	0.79*	-0.23^{ns}	**6**
						-	0.54*	0.91*	0.93*	0.55*	-0.18^{ns}	0.13^{ns}	**7**
							-	0.74*	0.67*	0.95*	0.57*	0.59*	**8**
								-	0.95*	0.77*	0.05^{ns}	0.42^{ns}	**9**
									-	0.69*	-0.11^{ns}	0.33^{ns}	**10**
										-	0.58*	0.46^{ns}	**11**
											-	0.24^{ns}	**12**
												-	**13**

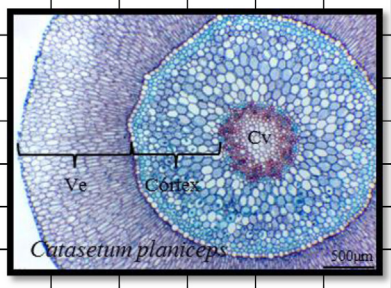

1. Root diameter (mm); 2. Root area in cross section (mm^2); 3. Velamen area in cross section (mm^2); 4. Area of vascular cylinder + cortex (mm^2) in cross section; 5. Number of layers of the velamen; 6. Thickness of velamen (μm); 7. Cortex thickness (μm); 8. Number of protoxylem strands; 9. Number of lignified cells of the exodermis; 10. Number of passage cells of the exodermis; 11. Number of lignified cells of the endodermis; 12. Number of passage cells of the endodermis; 13. Thickness of cell wall of the cells of the exodermis (μm). *Significant correlation at $p < 5\%$. ^{ns}Not significant.

nutrients flow inside the root. In the evaluated taxa there is a positive correlation between the number of vascular strands and the root diameter. Furthermore, the correlation between the number of vascular strands and the velamen area was significant. These results indicate that the *taxa* with smaller area of velamen, such as *Epidendrum nocturnum*, *Phalaenopsis cornu-cervie* and *Phalaenopsis hybrid* may compensate this smaller area for water absorption via velamen presenting greater number of xylem strands. Thus, there would be an increase in efficiency in water and solute transport for the remaining plant. This conclusion rests on the assumption of subsequent transfer of water and nutrients into living tissue. Our experimental approach is not suited to distinguish uptake into the velamen from transfer into living root tissue, let alone other plant compartments. However, previous work with entire plants has provided clear evidence for such a transfer (Zotz and Winkler, 2013).

Once the cells of velamen are dead at maturity, the water and nutrient transport in this tissue occurs in a passive way (Pita and Menezes, 2002). The number of cell layers of the velamen is strongly correlated with the thickness of this tissue, i.e. cell size does not very much. The velamen of orchids can have from one to 18 layers of cells (Solereder and Meyer, 1928; Engard, 1944). Although intraspecific variation in velamen thickness is generally considered to be small (Porembski and Barthlott, 1988), we observed some variation in spite of our small sample sizes, e.g. in the number of cell layers, the rate of maturation and cell size, or the patterns of parietal thickenings. Since the study plants were kept under very similar environmental conditions, this variation is probably related to genetic differences (Benzing et al., 1982).

The investment in the cortex and vascular cylinder directly leads to an increase in cell numbers in the exodermis. The lignified cells of the exodermis assume the role of an apoplastic barrier, and in conjunction with the velamen, offer mechanical protection and prevent water from returning from cortex to the external environment (Sanford and Adanlawo, 1973; Benzing et al., 1982; Ma and Peterson, 2003). The development of both O-thickenings and U-thickenings is associated with the deposition of suberin, cellulose and lignin (Ma and Peterson, 2003). The deposition of lignin in these cells can often obstruct the communication among them, reducing the cell lumina, and even leading to death.

In terrestrial plants, the root epidermis is in direct contact with the soil and plays a role in selective water and nutrient absorption (Barberon and Geldner, 2014). However, the dead cells of the velamen in roots transfer this selective function to the passage cells of the exodermis, via a symplastic path of entry into the root. In the endodermis, a more effective selection of substances occurs, and the passage cells are usually aligned with the poles of protoxylem, intensifying effectively the water flow (Peterson and Enstone, 1996; Moreira and Isaias, 2008). Thus, a larger number of passage cells in the endodermis can be a way to increase the water and nutrient inflow into the plant. Even though the root does not immobilize temporarily large amounts of fluids, by presenting little area of velamen, the passage of what was absorbed will be more rapid to vascular strands. In addition, the larger the number of xylem strands the faster the distribution of water and nutrients throughout the plant body. It is interesting to note that there is a positive correlation between velamen area and root diameter, but there is a much tighter correlation between the velamen area and the number of endodermis passage cells, indicating high efficiency for the water transport after its entry in the root.

The presence of cells with different types of wall thickenings in the cortex is typically interpreted as mechanical support (during desiccation) and water retention (Haberlandt, 1914; Olatunji and Nenguim, 1980). Among these, the phi-thickening consists of cellulose and lignin (and little or no suberin) (Wilcox, 1962), impregnated around the cell wall. In the studied taxa, phi-thickenings were located in the median layers of the cortical parenchyma, particularity of the type III phi-thickening (classification according to Van Tieghem, 1888). In spite of its similarity to the Casparian strips, phi-thickenings do not form an effective apoplastic barrier (Pires et al., 2003). The permeability of the phi-thickening was proven in several species of dicotyledons

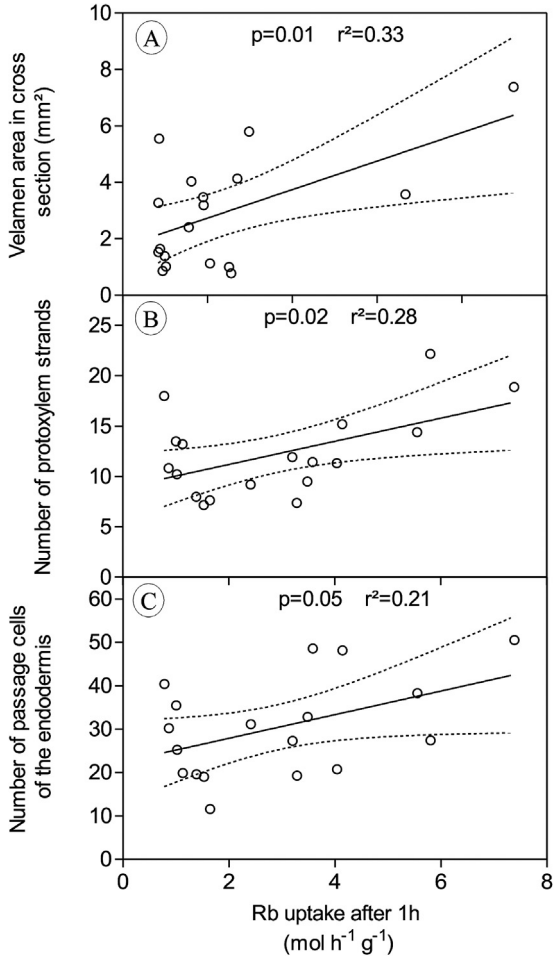

Fig. 4. Relationships of the rates of rubidium uptake (i.e. velamen adsorption and physiological uptake into the cortex) and anatomical characters of orchid roots. Data points are the mean values of 18 species. Solid lines show significant linear regressions, dotted lines show 95% confidence intervals.

(Perumalla et al., 1990) and in *Zea mays* (Degenhardt and Gimmler, 2000). Against this idea, studies with *Brassica oleracea* cultivated in environments with high salinity demonstrated effective selectivity for the movement of ions (Fernandez-Garcia et al., 2009). However, the discontinuity of these thickenings makes them ineffective as apoplastic barrier, reinforcing its role as mechanical support (Melo, 2011) and resistance to pressures exercised by other cells in expansion (Passioura, 1988). Another function of phi-thickening could be the prevention of the access of biological agents toward the central cylinder. Future studies should test whether there is a correlation between mechanical barriers and the invasion of fungi (Massicotte et al., 1988), or the relationship between the location of mycorrhizae and the occurrence of this type of thickening.

In contrast to phi-thickening, reticulate thickenings and uniform thickenings can assist the movement of substances to the vascular cylinder, contributing to the apoplastic flow (Stern and Judd, 2001), or act as mechanical support of the cortical parenchyma.

4.2. Nutrient absorption and it relationship with root structure

In aerial orchid roots, the flow of water and nutrients takes an apoplastic route in the velamen, whereas a symplastic route becomes mandatory in the passage cells of the exodermis. In the cortical parenchyma, the flow may again be (partially) apoplastic until reaching the next barrier, the endodermis. Here, water and nutrient passage into the vascular cylinder is again symplastic. The apoplastic route must also constitute a path for the mass flow and diffusion of water and nutrients via intercellular spaces and cell wall. The cell wall consists primarily of a chain of cellulose, hemicellulose and glycoproteins, in which the pectin matrix acts as moderator of cation exchange. The galacturonic acid monomers of pectins contain carboxylic groups (COO^-) with naturally negative charge and which work as agents of cation exchange. In this way, those monomers act as natural accumulators of cations in the apoplast, while the anions are repelled (Barberon and Geldner, 2014). For input of nutrients in the symplast, at some time, they must use specific plasma membrane transporters (Barberon and Geldner, 2014). The role of high pectin accumulation in cell walls in epiphytic roots can be compared with the colloidal properties of clay minerals in the soil around roots. The water and chemical affinity is generated because the clay minerals have a large electronegative surface contact, responsible for high cation adsorption capacity (Mergulies et al., 1988).

The rubidium ion is commonly used as analogue of potassium because potassium channels show a similar selectivity to this element as to the K^+ ion (Gierth and Mäser, 2007; Doyle et al., 1998). The positive charge of these ions suggests its high affinity for cell walls (pectins – COO^-) so that the velamen saturation (high pectic constitution of the cell wall) may have contributed to the significant correlation between velamen area and the absorption rates of Rb^+. When the velamen is saturated, the number of passage cells of the exodermis can limit or facilitate further absorption, depending on their density. The transporters and specific channels, in turn, guarantee the transcellular pathway and the entrance into the symplast through exodermis in radicular cortex. The endodermis and the vascular strands assume the role in directing ions flowing into the whole plant. In this case, after the prior exodermis selectivity, the cortical parenchyma may not be saturated as the velamen, and passage cells of the endodermis (aligned with the strands of xylem) would be more limiting to the transport of this ion.

Two points may have contributed to the lack of correlation between the anatomical characteristics and the rate of transport of the phosphorus radioisotope. First, the active process of absorption of phosphorous in plants, mediated by specific carriers (Santner et al., 2012); secondly, PO_4^{3-} is an ion considered of free access to roots when promptly available in nutrient solutions, since it presents negative charge and there are no restrictions to its transport to the interior of the cells (Santner et al., 2012).

5. Conclusions

The velamen is frequently depicted as an important structural feature of epiphytic orchids (and to lesser degree epiphytic aroids) for the absorption and retention of water and nutrients. However, there are very few studies that tried to relate characteristics of the velamen with other tissue types of aerial roots, let alone connect anatomical features with function. Our study shows that plants can differentially invest in larger proportions of different tissues, e.g. show a greater investment in strands of protoxylem and passage cells of the endodermis, specific thickenings in the cortical parenchyma that leads to proportional changes in symplastic and apoplastic flow of resources, i.e. water and nutrients. The correlation of the pectic constitution of velamen cells with nutrients absorption suggests that the passage of nutrients in the velamen does not entirely occur as free flow. The negative charge of the cell walls of the velamen will lead to temporary retention and subsequent gradual release of ions (especially cations). The suggested role of pectins in nutrient adsorption needs attention in orchids and other plants with a velamen such as many *Anthurium* species.

Funding

This work was supported by Fundação de Amparo à Pesquisa de Minas Gerais (APQ-656-11 and TAC Joca scholarship).

Acknowledgments

We acknowledge permits to export plant material from Panama, and thank the Botanical Garden of the University of Marburg (Germany) for supplying plant material.

References

Barberon, M., Geldner, N., 2014. Radial transport of nutrients: the plant root as a polarized epithelium. Plant Physiol. 166, 528–537.
Benzing, D.H., Friedman, W.E., Peterson, G., Renfrow, A., 1982. Shootlessness, velamentous roots and the preeminence of Orchidaceae in the epiphytic biotype. Am. J. Bot. 70, 121–133.
Benzing, D.H., 1990. Vascular epiphytes. In: General Biology and Related Biota. Cambridge University Press, Cambridge.
Benzing, D.H., 1996. Aerial roots and their environments. In: Waisel, Y., Eshel, A., Kafkafi, U. (Eds.), Plant Roots: The Hidden Half. Marcel Dekker, New York, pp. 875–894.
Benzing, D.H., 2000. Bromeliaceae: Profile of an Adaptive Radiation. Cambridge University Press, Cambridge.
Bukatsch, F., 1972. Bemerkungen zur Doppelfärbung: Astrablau-Safranin. Mikrokosmos 61, 255.
Chamberlain, C.J., 1932. Methods in Plant Histology. The University of Chicago Press, Chicago.
Degenhardt, B., Gimmler, H., 2000. Cell wall adaptation to multiple environmental stress in maize roots. J. Exp. Bot. 51, 595–603.
Doyle, D.A., Morais, C.J., Pfuetzner, R.A., Kuo, A., Gulbis, J.M., Cohen, S.L., Chait, B.T., MacKinnon, R., 1998. The structure of the potassium channel: molecular basis of K^+ conduction and selectivity. Science 280, 69–77.
Durrum, E.L., 1950. A microelectrophoretic and microionophoretic technique. J. Am. Chem. Soc. 72, 2493–2498.
Engard, C.J., 1944. Morphological identity of the velamen and exodermis in orchids. Bot. Gaz. 105, 457–462.
Esnault, A.L., Masuhara, G., McGee, P.A., 1994. Involvement of the exodermal passage cells in mycorrhizal infection of some orchids. Mycol. Res. 98, 672–676.
Fernandez-Garcia, N., Lopez-Perez, L., Hernandez, M., Olmos, E., 2009. Role of phi cells and the endodermis under salt stress in *Brassica oleracea*. New Phytol. 181, 347–360.
Gierth, M., Mäser, P., 2007. Potassium transporters in plants—involvement in K^+ acquisition, redistribution and homeostasis. FEBS Lett. 581, 2348–2356.
Haberlandt, G., 1914. Physiological Plant Anatomy, 4th ed. Mantagu Drumond, Mac-Millan, London.
Johansen, D.A., 1940. Plant Microtechnique. McGraw Hill Book Co., New York.
Kraus, J.E., Arduin, M., 1997. Manual básico de métodos em morfologia vegetal. Universidade Federal do Rio de Janeiro, EDUR, Rio de Janeiro.
Läuchli, A., Epstein, E., 1970. Transport of potassium and rubidium in plant roots: the significance of calcium. Plant Physiol. 45, 639–641.
Laube, S., Zotz, G., 2003. Which abiotic factors limit vegetative growth in a vascular epiphyte. Funct. Ecol. 17, 598–604.
Ma, F., Peterson, C.A., 2003. Current insights into the development, structure and chemistry of the endodermis and exodermis of roots. Can. J. Bot. 81, 405–421.
Massicotte, H.B., Peterson, R.L., Ackerley, C.A., Melville, L.H., 1988. Structure and ontogeny of *Betula alleghaniensis—Pisolithus tinctorius* ectomycorrhizae. Can. J. Bot. 68, 579–593.
Melo, H.C., 2011. Espessamento em fi de parede celular. Hoehnea 38, 1–7.
Mergulies, L., Rozen, H., Nir, S., 1988. Model for competitive adsorption of organic cations on clays. Clays Clay Miner. 36, 270–276.
Moreira, A.S.F.P., Isaias, R.M.S., 2008. Comparative anatomy of the absorption roots of terrestrial and epiphytic orchids. Braz. Arch. Biol. Technol. 51, 83–93.
Moreira, A.S.F.P., Lemos-Filho, J.P., Isaias, R.M.S., 2013. Structural adaptations of two sympatric epiphytic orchids (Orchidaceae). Rev. Biol. Trop. 61, 1053–1065.
Olatunji, O.A., Nenguim, R.O., 1980. Occurrence and distribution of tracheoidal elements in the Orchidaceae. Bot. J. Linn. Soc. 80, 357–370.
Passioura, J.B., 1988. Waster transport in and to roots. Annu. Rev. Plant Physiol. Plant Mol. Biol. 39, 245–265.
Perumalla, C.J., Peterson, C.A., Enstone, D.E., 1990. A survey of angiosperm species to detect hypodermal Casparian bands. I. Roots with a uniseriate hypodermis and epidermis. Bot. J. Linn. Soc. 103, 93–112.
Peterson, P.A., Enstone, D.E., 1996. Functions of passage cells in the endodermis and exodermis of roots. Physiol. Plant. 97, 592–598.
Peterson, C.A., 1988. Exodermal casparian bands: their significance for ion uptake by roots. Physiol. Plant. 72, 204–208.
Pires, M.F.O., Semir, J., Pinna, G.F.A.M., Felix, L.P., 2003. Taxonomic separation of the genera *Prosthechea* and *Encyclia* (Laeliinae: Orchidaceae) using leaf and root anatomical features. Bot. J. Linn. Soc. 143, 293–303.
Pita, P.B., Menezes, N.L., 2002. Anatomia da raiz de espécies de *Dyckia* Schult. f. e *Encholirium* Mart. ex Schult. & Schult. f. (Bromeliaceae Pitcairnioideae) da Serra do Cipó (Minas Gerais, Brasil), com especial referência ao velame. Revista Brasileira de Botânica 25, 25–34.
Porembski, S., Barthlott, W., 1988. Velamen radicum micromorphology and classification of Orchidaceae. Nordic J. Bot. 8, 117–137.
Pridgeon, A.M., 1987. The velamen and exodermis of orchid roots. In: Arditti, J. (Ed.), Rchid Biology. Reviews and Perspectives IV. Cornell University Press, Ithaca, New York, pp. 139–192.
Roland, J.C., Vian, B., 1991. General preparation and staining of thin sections. In: Hall, J.L., Hawes, E. (Eds.), Electron Microscopy of Plant Cells. Academic Press, London.
SPSS, 2000. Systat Version 10. SPSS Inc., San Francisco.
Sanford, W.W., Adanlawo, F.L.S., 1973. Velamen and exodermis characters of West African epiphytic orchids in relation to taxonomic grouping and habitat tolerance. Bot. J. Linn. Soc. 66, 307–321.
Santner, J., Smolders, E., Wenzel, W.W., Degryse, F., 2012. First observation of diffusion-limited plant root phosphorus uptake from nutrient solution. Plant Cell Environ. 35, 1558–1566.
Scatena, V.L., Nunes, A.C., 1996. Anatomia de *Pleurothallis rupestris* Lindl. (Orchidaceae) dos campos rupestres do Brasil, vol. 15. Boletim de Botânica da Universidade de São Paulo, pp. 35–43.
Solereder, H., Meyer, F.J., 1928. Systematische Anatomie der Monokotyledonen Heft III & VI. Gebrüder Bornträger, Berlin.
Stern, W.L., Judd, W.S., 2001. Comparative anatomy and systematics of *Catasetinae* (Orchidaceae). Bot. J. Linn. Soc. 136, 153–178.
Stern, W.L., 1999. Comparative vegetative anatomy of *Stanhopeinae* (Orchidaceae). Bot. J. Linn. Soc. 129, 87–103.
Trépanier, M., Lamy, M.-P., Dansereau, B., 2008. *Phalaenopsis* can absorb directly through their roots. Plant Soil 319, 95–100.
Tsavkelova, E.A., Cherdyntseva, T.A., Lobakova, E.S., Kolomeitseva, G.L., Netrusov, A.I., 2001. Microbiota of the Orchid rhizoplane. Microbiology 70, 492–497.
Van Tieghem, P., 1888. Le réseau de soutien de l'ecorce de la racine. Ann. Sci. Nat. Bot. Ser. 7/8, 375–378.
Went, F.W., 1940. Soziologie der Epiphyten eines tropischen Regenwaldes. Annales du Jardin Botanique de Buitenzorg 50, 1–98.
Wilcox, H., 1962. Growth studies of the root of incense cedar, *Libocedrus decurrens*: I. The origin and development of primary tissues. Am. J. Bot. 49, 221–236.
Withner, C.L., 1959. The Orchids: A Scientific Survey. Ronald Press Co., New York.
Zotz, G., Hietz, P., 2001. The physiological ecology of vascular epiphytes: current knowledge, open questions. J. Exp. Bot. 52, 2067–2078.
Zotz, G., Winkler, U., 2013. Aerial roots of epiphytic orchids: the velamen radicum and its role in water and nutrient uptake. Oecologia 171, 733–741.
Zotz, G., 2013. The systematic distribution of vascular epiphytes—a critical update. Bot. J. Linn. Soc. 171, 453–481.